# Chapter 1: Introduction

## 1.1. Overview

Atmospheric aerosols are known to influence climate. For example, Plutarch noted that eruption of Mt. Etna in 44 B.C. may have been the primary reason that crops did not grow the following summer and for subsequent famines in Rome and Egypt. Benjamin Franklin suggested that a volcanic eruption in Iceland in 1783 may have been responsible for an abnormally cold summer and winter that ensued, while the 1815 volcanic eruption at Tambora resulted in a "year without summer" [*Robock*, 2002]. In 1883, the eruption at Krakatoa, Indonesia, spewed a plume of volcanic dust that caused the "volcanic sunsets" reported in London [*Robock*, 2002]. More recently, eruptions at El Chichon in Mexico (1982) and Mt Pinatubo in the Philipines (1991) produced large amounts of stratospheric aerosol that had lingering effects. Tropospheric sulfate aerosols are believed to be crucial in the modulation of the earth's greenhouse effect [*Graf et al.*, 1997].

The high sulfate aerosol concentrations that are introduced into the stratosphere by major volcanic eruptions tend to increase Earth's albedo, and hence, the temperature of the stratosphere, by several K, and cause marked decreases in tropospheric temperatures [*Pueschel*, 1995].

Even in the absence of volcanic input, a perennial stratospheric sulfate aerosol exists which plays a critical role in the heterogeneous chemistry that leads to ozone depletion during the polar spring. In the cold polar winter, $HNO_3$ and water vapor condenses on preexisting stratospheric aerosols, enhancing the rate of ozone loss by removal of the stratospheric $NO_x$ species, which act as scavengers of reactive chlorine,

and at the same time, provide catalytic surfaces for reactivation of "inert" chlorine bound in the form of HCl and $ClONO_2$.

The exact origins of background stratospheric sulfate aerosol (SSA) have been a subject of debate since the first modern accounts of stratospheric sulfate aerosols were reported by *Junge et al.* [1963], who documented the results of measurements using Aitken nuclei counters and impactors of an aerosol population with a maximum diameter between 0.01 and 0.10 μm. Substantive developments in measurement techniques and numerous measurements of stratospheric aerosols and PSC (polar stratospheric cloud) particles have been made in the intervening years by a variety of techniques [*Pantani et al.*, 1999], on a variety of platforms, ranging from ground-based instruments to balloon or satellite borne ones [*Hervig and Deshler*, 2002]. For example, *Hofmann et al.*, [1998], operating out of Laramie, Wyoming, have compiled data from balloon-borne collectors since the 1970s, and from measurements of a variety of aerosol characteristics such as number concentration, surface area, mass density, and optical thickness that have been made using NASA satellites such as the Stratospheric Aerosol Measurement (SAM I & II) and Stratospheric Aerosol and Gas Experiment (SAGE I & II) instruments. The satellite data provides the most comprehensive database on the SSA layer.

More recently, there has been intense interest in the effects of anthropogenic activity such as aircraft and industrial sulfur emissions on Stratospheric Sulfate Aerosol (SSA) levels [*Hofmann*, 1991; *Lukachko et al.*, 1998; *Pitari et al.*, 2002].

There have also been significant advances in our knowledge of the thermodynamics of sulfate aerosol systems, both tropospheric and stratospheric [*Carslaw et al.*, 1995; *Carslaw et al.*, 1997; *Clegg and Brimblecombe*, 1995; *Clegg et al.*, 1998;

*Michelson*, 1998; *Steele and Hamill*, 1981]. Nevertheless, fundamental questions regarding the origins of SSA particles remain unanswered.

*Junge et al.* [1963] postulated that 1) SSA particles smaller than 0.1 μm were of tropospheric origin, 2) larger particles were probably of extraterrestrial origin [*Junge et al.*, 1961], and 3) those between 0.10 and 1 μm were formed in the stratosphere, possibly by oxidation of $H_2S$ or $SO_2$. However, because $H_2S$ and $SO_2$ are rapidly oxidized in the troposphere, concentrations of either compound in the upper reaches of the troposphere are relatively low. Thus, carbonyl sulfide (OCS), which is relatively unreactive in the troposphere, has been proposed to be the major source of the background stratospheric sulfate aerosol [*Crutzen*, 1976]. Uncertainties in the atmospheric sulfur budget, [*Chin and Davis*, 1995; *Watts*, 2000], coupled with difficulties in the collection and measurement of actual levels of background SSA particles [*Thomason et al.*, 1997], make it difficult to assess the extent to which OCS contributes to the sulfate loading.

Measurements on single particles have shown evidence of extraterrestrial materials in a large fraction of aerosol particles, as well as significant amounts of organic matter in high tropospheric aerosols [*Murphy et al.*, 1998]. Because of the low amount of extraterrestrial sulfur accreted by the earth [*Love and Brownlee*, 1993], it is unlikely that a significant amount of the SSA sulfate could be of extraterrestrial origin (although the contribution of meteoretic sulfur in the upper atmosphere may be appreciable). These results suggest that the processes by which aerosols and their precursors are produced and transported in the stratosphere are complex.

*Chin and Davis* [1995] showed using a simple 1-D model that the available atmospheric OCS levels are inadequate to maintain the SSA population. Other studies

indicate that other significant sources of stratospheric sulfate [*Kjellstrom*, 1998; *Weisenstein et al.*, 1997], such as $SO_2$ from the lower troposphere, are transported upwards by deep-convective events. Many models of the chemistry and physics of the Junge Layer are consistent with the need to invoke additional sulfur sources. [*Chin and Davis*, 1995; *Golombek and Prinn*, 1993; *Kjellstrom*, 1998; *Pitari et al.*, 2002; *Timmreck*, 2001; *Weisenstein et al.*, 1997]. SSA chemistry and microphysics have been explicitly treated in a multi-year GCM (general circulation model) run [*Timmreck*, 2001], while *Pitari et al.* [2002] used a 3-D chemical transport model to apportion the relative contributions of OCS photolysis, $SO_2$ oxidation, and uplifted $H_2SO_4$. Their models suggest the distribution to be 43%, 27%, and 30 % of total SSA mass, respectively [*Pitari et al.*, 2002; *Timmreck*, 2001]. However, the variability in the observed profiles of $SO_2$ and gas phase $H_2SO_4$ precludes model validation. Moreover, the design of GCMs makes them incapable of simulating certain trends in SSA concentrations (for example, the effect of the QBO, quasi-biennial oscillation [*Timmreck*, 2001].) Given our limited knowledge of the fundamental characteristics of the background SSA [*Thomason et al.*, 1997] and persistent uncertainties in available models, other approaches are required.

An alternative approach to this problem involves the used of specific isotopic signatures of sulfur. Isotopic methods have been used to tackle a wide variety of geophysical problems in atmospheric chemistry and global transport. HDO and $H_2{}^{18}O$, for example, have been used to study precipitation and the tropospheric/stratospheric water budget [*Hoffmann et al.*, 2000; *Jouzel et al.*, 1991].

The isotopic composition of SSA particles should reflect the isotopic composition of their various sources, and the mechanisms of formation [*Krouse and Grinenko*, 1991;

*Rahn and Wahlen*, 1997; *Rahn and Wahlen*, 2000]. Data on the isotopic com position of atmospheric OCS and of SSA particles should be able to constrain the OCS loss mechanisms and its relative contribution to background stratospheric sulfate [*Goldman et al.*, 2000].

Isotopic methods have been used to study the effects of volcanic events on stratospheric aerosols for more than 30 years. [*Castleman et al.*, 1973; *Castleman et al.*, 1974; *Forrest and Newman*, 1973; *Forrest and Newman*, 1977; *Lazrus et al.*, 1971]. However, specific sulfur isotopic fingerprinting has been used primarily to trace sources of tropospheric aerosols [*Krouse and Grinenko*, 1991], although its use has been limited because of an incomplete understanding of isotopic effects of atmospheric processes and the lack of data on sulfur isotopic abundances of sulfur compounds in the atmosphere.

To take advantage of sulfur isotopic tracing, we need 1) more data about specific isotopic compositions; and 2) a better understanding of isotopic substitution on environmentally important physical and chemical processes.

**1.2 Outline**

The photodissociation of OCS in the stratosphere and the oxidation of tropospheric $SO_2$ by OH are considered two of the most important pathways for maintaining stratospheric sulfate levels. In Chapters 2, 3, and 4, I quantify the effects of isotopic substitution on these reactions using theoretical and experimental methods. In Chapter 2, I present the results of our analysis of high-resolution FTIR spectra from the Caltech/JPL MkIV instrument of OCS isotopologues, which gives us a handle on the apparent isotopic enrichment of OCS in the stratosphere and on the sulfur isotopic

composition of OCS-derived stratospheric aerosols. In Chapter 3, the effect of isotopic substitution on the rate of $SO_2$ oxidation by OH is estimated using RRKM theory of unimolecular decomposition [*Robinson and Holbrook*, 1972]. In Chapter 4, I examine the effect of isotopic substitution on the photolysis of OCS by analyzing the effects of sulfur isotopic substitution on the UV absorption spectra of $OC^{32}S$ and $OC^{34}S$.

In Chapter 5, I present the results of a modeling study of stratospheric sulfur species that are based on using the JPL/NASA KINETICS chemical transport model (CTM) and the isotopic data from Chapters 2-4. From this model, I predict the expected isotopic composition of SSA particles and of important sulfur-containing precursors.

Major findings are summarized in Chapter 6. The sulfur isotopic composition of SSA particles is consistent with the hypothesis that $SO_2$ and OCS are the most significant contributors of stratospheric sulfur. Discrepancies between the predicted and measured sulfur compositions of SSA particles can be due in part to inadequacies in our model.

The preliminary results from our analysis of stratospheric filter samples collected during an aerosol loading minimum are presented in Appendix A and corroborate the previously published results of Castleman et al. [*Castleman et al.*, 1973; *Castleman et al.*, 1974].

This work represents the first attempt to constrain the sources of stratospheric sulfate aerosol using isotopic constraints.

## 1.3 Background

### 1.3.1 Atmospheric sulfur compounds

The most abundant sulfur-based gases in the atmosphere are hydrogen sulfide $H_2S$), dimethyl sulfide ($CH_3SCH_3$), carbon disulfide ($CS_2$), carbonyl sulfide (OCS) and

sulfur dioxide ($SO_2$). They are all subject to indirect photochemical oxidation by variety of atmospheric species including hydroxyl radicals, ozone, and excited oxygen atoms, and to direct photochemical decomposition. The ultimate fate of these atmospheric sulfur compounds is the irreversible oxidation to sulfate ($SO_4^{2-}$), the major constituent of tropospheric and stratospheric sulfate aerosols (i.e., $H_2SO_4$, $NH_4HSO_4$, $(NH_4)_2SO_4$).

The above atmospheric sulfur compounds have a variety of natural and anthropogenic sources. The major sources and sinks of sulfur compounds are summarized in Table 1.1. The total anthropogenic source strength is roughly two or three times larger than total natural emissions. There is considerable uncertainty associated with natural sources. Anthropogenic emissions are primarily in the form of $SO_2$ from combustion of fossil fuels, while biogenic DMS comprises the majority of natural emissions, excluding sea-salt sulfate.

**Table 1.1: Global sources of sulfur (Tg-S/year)**

| Source | $H_2S$ | $CH_3SCH3$ | $CS_2$ | OCS | $SO_2$ | $SO_4$ | Total |
|---|---|---|---|---|---|---|---|
| Fossil fuel combustion and industry | | Total reduced sulfur = 2.2 | | | 70 | 2.2 | 71-77 (in the mid 1980's) |
| Biomass burning | < 0.01 | | < 0.01 | 0.075 | 2.8 | 0.1 | 2.2-3.0 |
| Oceans | <0.3 | 15-25 | 0.08 | 0.08 | | 40-320 | 15-25 |
| Wetlands | 0.006-1.1 | 0.003-0.68 | 0.0003-0.06 | | | | 0.01-2 |
| Plants and soils | 0.17-0.53 | 0.05-0.16 | 0.02-0.05 | | | 2.4 | 0.25-0.78 |
| Volcanoes | 0.5-1.5 | | | 0.01 | 7-8 | 2-4 | 9.3-11.8 |
| Anthropogenic (total) | | | | | | | 73-80 |
| Natural (total – sea salt – soil dust) | | | | | | | 25-40 |
| Total | | | | | | | 98-120 |

Table 1.1 adapted from Seinfeld and Pandis, 1997.

### 1.3.2 Global sources and sinks of atmospheric carbonyl sulfide

OCS is the sulfur species which is most resistant to oxidation in the troposphere. For example, it accounts for more than 80% of gas-phase sulfur above 8 km (Farwell, 1995). It is produced from the oxidation of DMS and $CS_2$, and is also directly emitted from oceans as a byproduct of biological and photochemical reactions, which account for 13%, 32, and 22% of the global sources, respectively. Since OH oxidation of more reduced sulfur species accounts for a significant fraction of atmospheric OCS, OCS concentrations show both marked diurnal and seasonal dependencies [*Griffith et al.*, 1998; *Pueschel*, 1995].

According to current estimates, soils act as a net sink of OCS. However, a particular soil environment may constitute either a sink or a source depending on whether

the soil is anoxic or oxic. When the soil is anoxic, it acts as an OCS source; and when a soil is oxic, it acts as a net sink. Net OCS emissions from anoxic soils have been estimated to be 0.02 +/- 0.01 Tg/a, while uptake by oxic soils appears to be a major sink at 0.92 +/-0.78 Tg/a. The large uncertainties in the above estimates cast doubt on the actual role of soil vis-à-vis the global OCS budget. Uptake by vegetation (0.56+/- 0.10 Tg/a) appears to be another large sink for OCS.

OCS is resistant to photolysis at wavelengths found in the troposphere (i.e., ≥ 290 nm) and its chemical lifetime at typical tropospheric OH concentrations (e.g., $10^5$ molec $cm^{-3}$) is on the order of 17 years. Its mixing ratio in the troposphere remains relatively constant with altitude at 500 pptv up to the tropopause. However, OCS absorbs strongly at wavelengths < 290 nm, with an absorption maximum at ~223 nm, and that it photolyzes rapidly above the ozone layer. Oxidation by OH and O (0.02 +/- 0.01 Tg/a, and 0.03 +/- 0.01 Tg/a, respectively, compared to 0.13 +/- 0.1 Tg/a for the photodissociation of OCS) account for the remainder of stratospheric OCS loss, according to one model estimate [*Chin and Davis*, 1995]. The OCS that is transformed in the stratosphere ultimately ends up as stratospheric sulfate aerosol (SSA) via oxidation to $SO_2$ and subsequently to $H_2SO_4$.

*Chin and Davis* [1993] estimated the direct anthropogenic emissions of OCS to be ~0.04+-0.2 Tg/a. In a later study, *Watts* [2000] updated this earlier estimate to include the direct emissions from aluminum production, such that the revised estimate of the anthropogenic OCS source term is 0.12 +/- 0.06 Tg/a.

The considerable uncertainties concerning the importance of different OCS sources precludes the OCS budget from self-consistency. For example, the uncertainty is

on the same order of magnitude as the total sources and sinks (i.e., 0.34 +/- 0.84 Tg/a, compared to 1.31+/- 0.25 Tg/a for total sources and 1.66+/- 0.79 Tg/a for total sinks) [*Watts*, 2000].

*Chin and Davis* [1995] estimated that the total atmospheric OCS loading to be 5.2 Tg, with 4.6 Tg in the troposphere and 0.57 Tg in the stratosphere. Combining their data with Watt's estimate of a global OCS source strength of 1.31 Tg/a, the overall lifetime of OCS in the atmosphere is ~ 4 years.

### 1.3.3 Sources and sinks of sulfur dioxide and sulfate

Based on the work of *Chin and Davis* [1995], OCS is no longer considered to be the single most important source of stratospheric sulfur. Another primary source is tropospheric $SO_2$ injected through the tropopause by deep-convection in the ITCZ (inter-tropical convergence zone) [*Kjellstrom*, 1998; *Pitari et al.*, 2002; *Timmreck*, 2001]. Anthropogenic sulfur pollution associated with automobiles and industrial activity comprises the majority of sulfur dioxide emissions. Total annual $SO_2$ emissions have been estimated to be 80 Tg-S/A, of which 70 Tg-S is attributed to fossil fuel burning and industrial sources. The remainder originates from biomass burning and volcanic activity [*Seinfeld and Pandis*, 1998]. As previously mentioned, volcanic plumes advected through the tropopause provide a large influx of sulfur to the stratosphere, primarily in the form of $SO_2$. $SO_2$ is transformed primarily via gas-phase oxidation by OH in the stratosphere, and by heterogeneous oxidation in cloudwater by $O_3$, $H_2O_2$, and metal-catalyzed oxidation by $O_2$ in the troposphere. Because $SO_2$ has a short tropospheric lifetime on the order of about a week in a well-mixed atmosphere at typical OH

concentrations and tropospheric aerosol loading, $SO_2$ concentrations in the boundary layer vary significantly, from about 20 pptv in remote areas to over 300 ppbv in polluted urban areas [*Seinfeld and Pandis*, 1998].

Sulfate in the troposphere is also produced during the oxidation of other sulfur containing species such as $CS_2$, DMS, $H_2S$, RSH, and DMSO. Tropospheric sulfate loading is higher in the summer, due to more efficient oxidation of $SO_2$ by OH and heterogeneously by $H_2O_2$ in clouds [*Seinfeld and Pandis*, 1998], and like most other sulfur compounds, is more pronounced in the northern than the southern hemisphere.

### 1.3.4. Properties of the background stratospheric sulfate layer

The characteristics and origin of the stratospheric sulfate aerosol (SSA) layer have been the subject of numerous studies since in was first described by *Junge et al.* in 1961 [*Crutzen*, 1976; *Turco et al.*, 1980]. The SSA layer helps to regulate the albedo of Earth's atmosphere, and also plays a crucial role in the chemistry at high altitudes. Among other roles, SSA catalyzes heterogeneous reactions that recycle the inert halogen species governing the ozone budget: nitrogen oxides are converted into nitric acid on SSA [*Griffith et al.*, 2000; *Rahn and Wahlen*, 1997].

Volcanic eruptions represent a major perturbation to and are the major contributor of stratospheric sulfate sulfur, increasing the SSA number concentration by up to several orders of magnitude. During volcanically quiescent periods, a persistent SSA layer has been observed extending from above the tropopause to about 30 km high, with a maximum around 20 km, although there has been persistent uncertainty regarding true background aerosol levels [*Hitchman et al.*, 1994]. There has also been considerable

debate around the origin of particle nuclei. Recent single particle studies of stratospheric particles have suggested that some nuclei have an extraterrestrial source [*Murphy et al.*, 1998].

Observations from SAGE II show a background SSA layer that is roughly symmetrical in the northern and southern hemispheres. The particle number density in this liquid aerosol layer varies between 1 and 10 particles $cm^{-3}$, the surface area density between 0.1 and 1.0 $\mu m^2 cm^{-3}$, and mass loading between 0.1 and 1.0 $\mu g\ m^{-3}$ [*Yue et al.*, 1994], depending on the height and latitude. The particle population is generally described as being unimodal, with the log of the particle size distributed normally around ~0.07 um [*Hamill et al.*, 1997]. Figure 1.1 shows the decadal averages of SSA surface area, including volcanic effects, and encapsulates the important chemical reactions that produces SSA sulfate. During the polar winter, $HNO_3$ and water vapor condense on preexisting SSA particles and form liquid, ternary solutions of $HNO_3$, $H_2SO_4$ and $H_2O$ (~190-195 K). The ternary liquid aerosols absorb even more $HNO_3$ and $H_2O$ as temperatures decrease (188-190 K), eventually leading to binary $HNO_3/H_2O$ mixtures, which crystallize to form NAT (Nitric acid trihydrate) particles [*Seinfeld and Pandis*, 1998].

The stratospheric sulfate burden is estimated from SAGE II data at 0.156 Tg-S [*Pitari et al.*, 2002]. *Weisenstein et al.* [1997] estimated the lifetime of background SSA particles to be 1.2 years. However, that estimate was made using model results that put the stratospheric sulfate aerosol burden at about 0.087 Tg-S and the sulfate production rate at 71 kT-S/yr. Those estimates have since been revised to be more in line with the SAGE derived estimate [*Pitari et al.*, 2002; *Weisenstein*, 2002]. The most recent

estimate of the SSA lifetime is ~3-4 years, which is considerably longer than previously believed [*Turco et al.*, 1982; *Turco et al.*, 1980], and about the same as the lifetime for OCS.

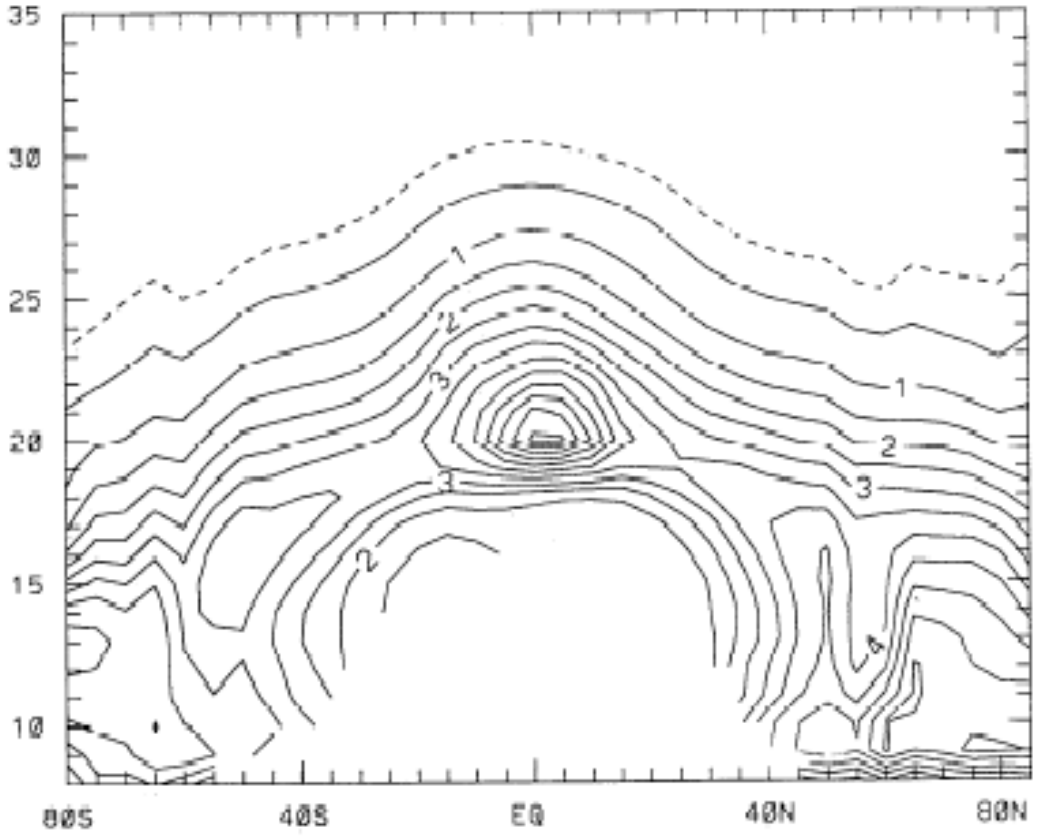


**A.**

$$SO_2 + OH + M \rightleftharpoons HOSO_2 + M$$
$$HOSO_2 + O_2 \rightarrow HO_2 + SO_3$$
$$SO_3 + 2\,H_2O \rightarrow H_2SO_4 \cdot H_2O$$

**B.**

$$SO_2 + H_2O \rightleftharpoons H^+ + HSO^{3-}$$
$$S(IV) \xrightarrow{H_2O_2,\ O_2/Fe(III)/Mn(II),\ O_3,\ NO_3^-} S(VI)$$

**C.**

$$OCS \xrightarrow{h\nu} CO + S$$
$$S + O_2 \rightarrow SO + O$$
$$S + O_3 \rightarrow SO + O_2$$
$$S + OH \rightarrow SO + H$$
$$SO + OH \rightarrow SO_2 + H$$

**Figure 1.1:** Decadal average surface area in $\mu m^2\ cm^{-3}$ for 9.1 years of SAGE II and SAM II data (1979-1981 and 1984-1990), adapted from *Hitchman et al.,* [1994] and summary of synopsis of important $SO_2$ (A: homogeneous, B: heterogeneous) and OCS chemistry (C) in the production of stratospheric sulfate. Atmospheric heterogeneous sulfur chemistry is discussed in detail in the appendices.

The composition of the aerosol droplets depends on ambient temperature and relative humidity, with the sulfate fraction varying between 40 and 90%. A typical aerosol particle has a $H_2SO_4$ fraction of ~75%, with water making up the remainder.

As temperatures decrease, water is condenses and constitutes a growing fraction of the aerosol. In the polar stratosphere, the vapor pressure of $HNO_3$ is sufficiently suppressed that condensed nitric acid becomes a major component of the aerosol. The combination of elevated freezing point and lowered temperatures results in formation of crystalline, non-spherical, PSCs (polar stratospheric clouds) or ternary $H_2SO_4/HNO_3/H_2O$ liquids which are critical to the stratospheric processes that cause the "ozone hole" observed in polar regions [*Seinfeld and Pandis*, 1998].

Carbonyl sulfide was for many years believed to be the immediate precursor to background stratospheric sulfate [*Crutzen*, 1976; *Turco et al.*, 1980]. As previously noted, OCS is fairly unreactive in the troposphere, and therefore it is the sulfur compound that exists at the highest concentrations at the tropopause [*Farwell et al.*, 1995]. The other atmospherically-relevant sulfur species have appreciably shorter tropospheric lifetimes. Even though OCS is a plausible precursor of background SSA, the extent of its contribution cannot be assessed solely from budget considerations, given the uncertainties associated with global OCS sources and sinks [*Chin and Davis*, 1995; *Watts*, 2000]. Several research groups suggested that the net sulfur influx of tropospheric OCS is insufficient to maintain steady-state SSA levels [*Chin and Davis*, 1995; *Kjellstrom*, 1998], and that elevated $SO_2$ levels at the tropopause caused by deep convective events at the tropics should be considered to be a major contributor to SSA [*Weisenstein et al.*, 1997].

The latest models estimate that 43% of SSA particles originate from OCS photolysis, 30% from upwardly transported sulfate and 27% from $SO_2$ oxidation [*Pitari et al.*, 2002; *Timmreck*, 2001]. However, it is apparent that model studies of the SSA layer are clearly deficient in many respects. Even though OCS and $SO_2$ concentration vs. altitude profiles have been determined at specific locations, the total database is sparse, and it is therefore very difficult to validate any model predictions. Furthermore, transport may play a more important role in the overall aerosol budget than previously assumed. For example, at present there are significant differences among the 2-D and 3-D models that have been developed [*Timmreck*, 2001].

Further insight into the origins of the background stratospheric sulfate layer will ultimately allow us to better understand the effects of anthropogenic activity on stratospheric chemistry.

Recent data and models clearly indicate that $SO_2$ is a more significant source of stratospheric sulfate than previously believed; and since anthropogenic activity represents a dominant source of $SO_2$, it is possible that our activities have greater impact on stratospheric aerosols than previously believed [*Pitari et al.*, 2002]

## 1.4 Isotopic effects and the isotopic composition of atmospheric sulfur

### 1.4.1 Expressing isotopic composition

The contribution of OCS and other species to the SSA layer should be reflected in the isotopic characteristics of the particular sulfur sources, the isotopic characteristics of

the resultant SSA particles, and the isotopic fractionation associated with the chemical and physical processes that produce them.

There are four stable sulfur isotopes: $^{32}S$, $^{33}S$, $^{34}S$, and $^{36}S$ that occur in natural abundances of about 95, 0.75, 4.2, and 0.017% respectively [*Krouse and Grinenko*, 1991]. Differences among the isotopic abundances of sulfur compounds are generally small. These differences are usually expressed relative to a standard, defined for $^{34}S$ as:

$$\delta^{34}S = 1000 \times \left[ \frac{(^{34}S/^{32}S)_{sample}}{(^{34}S/^{32}S)_{standard}} - 1 \right] \quad (1.1)$$

The unit for δ is ‰ ("per mil"). A similar expression can be written for any pair of isotopologues. The value of the standard for $^{34}S/^{32}S$ is set, by convention, to 1/22.22, the isotopic abundance of Canyon Diablo meteorite [*Krouse and Grinenko*, 1991]. Because planetary bodies and meteorites are believed to have a similar cosmic source of homogeneous isotopic composition, the isotopic composition of meteorites reflects, roughly, the average isotopic composition of total terrestrial sulfur. Deviations from $\delta^{34}S$ = 0 ‰ arise from the isotopic fractionation that accompanies chemical and physical processing.

### 1.4.2 Isotopic fractionation processes

Isotopic fractionation processes fall into two broad categories, equilibrium or kinetic. In either case, fractionation is often expressed in terms of an isotopic enrichment factor:

$$\varepsilon = (\alpha - 1)*1000 \quad (1.2)$$

where $\alpha$ is either the equilibrium isotopic ratio, or the ratio of the kinetic rate constants, between the heavy and parent isotopologues, associated with a particular process. In the case of sulfur isotopologues/isotopomers, $^{32}S$ is used as the reference isotope (isotopomers are isotopologues that are structural isomers). The symbol $\Delta$ refers to the isotopic discrimination factor [*Farquhar et al.*, 1989]. However, especially in studies of complicated systems such as ecosystem gas-exchange, $\Delta$ is often taken to be the weighted isotopic fractionation factor associated with the overall process, rather than the kinetic or equilibrium enrichment factor associated with a specific process [*Yakir and da Silveira Lobo Sternberg*, 2000]. In addition, there is the added ambiguity of $\Delta$ being used to represent an anomalous trend which has been referred to as mass-independent isotopic fractionation. For clarity and convenience, we will use the symbol $\varepsilon$ throughout this work.

By convention, a *normal kinetic isotope effect* is one in which the heavy isotope is discriminated against (i.e., the product is depleted in the product, $k_{light} > k_{heavy}$). In an *inverse kinetic isotope effect*, $k_{light} < k_{heavy}$, and the product is enriched in the heavy isotope. *Primary isotope effects* refer to those isotopic effects in which the isotopically-substituted atom is directly involved in the reaction. *Secondary isotope effects* refer to an isotopic effects caused by a change in the density of states due to the isotopic substitution [*Robinson and Holbrook*, 1972].

Equilibrium isotopic effects may result from isotopic exchange between two sulfur-containing species. An example is the exchange reactions between $H_2S$ and $SO_2$:

$$H_2{}^{32}S + {}^{34}SO_2 \leftrightarrow H_2{}^{34}S + {}^{32}SO_2 \qquad (1.3)$$

The equilibrium constant for this reaction can be expressed in terms of the partition functions of the individual compounds:

$$K_{eq} = \frac{Q(H_2{}^{34}S)Q({}^{32}SO_2)}{Q(H_2{}^{32}S)Q({}^{34}SO_2)} \quad (1.4)$$

The ratio of the partition functions can be expressed purely in terms of the vibrational frequencies of the reacting molecules [*Weston*, 1999]. The isotopic fractionation of reversible reactions can therefore be calculated conveniently.

In some cases, the isotopic fractionation associated with the heterogeneous oxidation of $SO_2$ to $SO_4^{2-}$ is controlled by the phase change reaction:

$$^{32}SO_{2(g)} + {}^{34}SO_3{}^{2-}{}_{(l)} \leftrightarrow {}^{34}SO_{2(g)} + {}^{32}SO_3{}^{2-}{}_{(l)} \quad (1.6)$$

which precedes the more rapid, and essentially complete, oxidation of $HSO_3^-$ to $SO_4^{2-}$ by $H_2O_2$, $O_3$, or by catalytic auto-oxidation. The isotopic fractionation rate for this process has been estimated to be about 1.02, but experimental estimates have generally higher values [*Krouse and Grinenko*, 1991].

Other kinetic isotopic fractionation effects are associated with reductive or oxidative reactions, such as the reduction of $SO_4^{2-}$ to $HS^-$. Yet others are caused by isotopologues being photolyzed at different rates because of subtle differences in the absorption cross-sections of isotopologues. *Yung and Miller* [2001] propose a general theory based on differences in the zero point energy (ZPE) of substituted species to estimate the magnitude and sign of these effects. This theory is able to predict the sign but not the magnitude of the apparent enrichment of stratospheric $N_2O$ [*Griffith et al.*, 2000]. It remains unresolved whether a general "rule of thumb" is applicable to all or to even the majority of cases, although substantial progress has been made in our

understanding of the effect of isotopic substitution on the absorption cross-sections of isotopically-substituted triatomic species [*Johnson et al.*, 2001; *Miller and Yung*, 2000; *Weston*, 1999; *Yung and Miller*, 1997; *Zhang et al.*, 2000].

Kinetic isotopic fractionation effects of chemical processes such as the oxidation of $SO_2$ by OH can be calculated on the basis of transition state theory, where the reactant molecules are assumed to be in equilibrium with an activated complex.

For convenience and simplicity, it has often been assumed that the most important effect of substitution with a heavier isotope is the lowering of ground-state vibrational energy levels (i.e., *a primary isotope effect*). The consequence of this would be that the activation energy for the lighter isotopes would be lower, and thus they should react faster, resulting in a depletion of the lighter isotopes in the reactant pool and a corresponding enrichment in the reaction product [*Canfield*, 2001]. In reality, the situation is considerably more complicated, since isotopic substitution changes the energy levels of the excited states and the population of these states as well as those of the ground state (*secondary isotope effects*). The sign and magnitude of isotopic fractionation may therefore depend critically on the properties of the transition state.

### 1.4.3. Isotopic fractionation as Rayleigh distillation processes; open and closed systems

Some environmental systems involving kinetic isotopic fractionation processes can be described in terms of a Rayleigh distillation process, in which a finite pool of two or more reactants are irreversibly depleted at different rates [*Rahn and Wahlen*, 1997]. For an irreversible process, where A and B are two species being lost at different rates:

$$A = A_0 e^{-k_A t} \quad (1.7)$$

$$B = B_0 e^{-k_B t} \quad (1.8)$$

and

$$A/B = A_0/B_0 e^{-(k_A - k_B)t} \quad (1.9)$$

We furthermore assume a diffusive atmosphere where A and B have an irreversible stratospheric sink and are both being carried upward at a uniform rate. We define B be the more abundant species, and define the following quantities:

$$\alpha = k_A/k_B \quad (1.10)$$

$$\varepsilon' = \alpha - 1 \quad (1.11)$$

Using the defined quantities and defining a ratio R=A/B, we can obtain:

$$\ln R - \ln R_o = \varepsilon' \ln(f) \quad (1.12)$$

For atmospheric gaseous species, such as OCS and $N_2O$, where $\delta$ is small and $\varepsilon$ is constant, by first taking the first term of the Taylor series expansion of ln R and ln $R_o$, and then converting all quantities to ‰ units, the following approximation can be made:

$$\delta = \delta_o + \varepsilon \ln(f) \quad (1.13)$$

where $\varepsilon$ is the isotopic enrichment factor in ‰, *f* is the fraction of substrate remaining, and $\delta_o$ is the initial value for the substrate [*Rahn and Wahlen*, 1997]. As illustrated in Figure 1.2, differences in the value of $\delta$ between the reactant and product species in a kinetic process depend on both the isotopic enrichment factor ($\varepsilon$) and the extent of fractionation (*f*). The initial product $\delta$ is offset from that of reactant by the isotopic enrichment factor, $\varepsilon$. However, as the reaction proceeds, the reactant will become increasing either depleted or enriched in the heavier isotope. At the same time, the value

of δ for the product will approach that of the reactant before the reaction began ($\delta_o$). At 100% conversion the product will obviously have exactly the same value of δ as the reactant originally, as illustrated in the example below, while the reactant δ will approach ∞ (-∞).

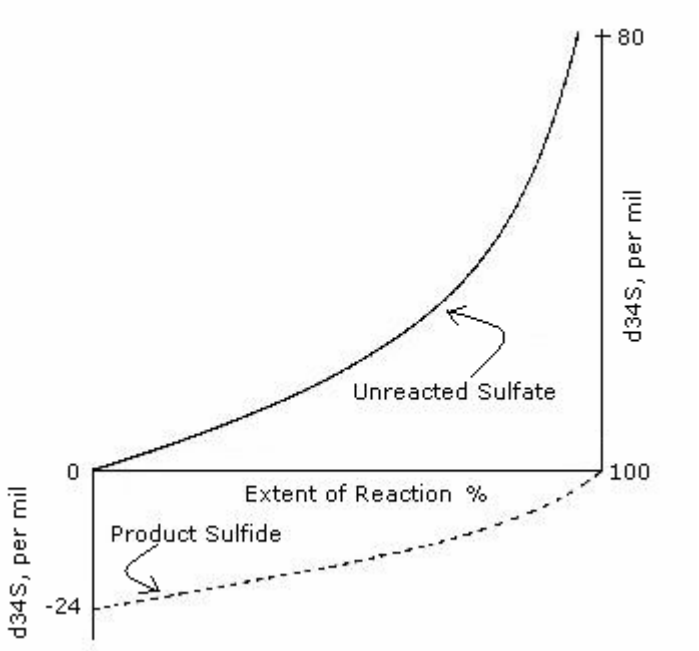


**Figure 1.2**: Changes in the $\delta^{34}S$ of reactant sulfate and product sulfide as a function of the extent of reaction, where $^{32}SO_4^{2-}$ is reduced 1.024 faster than $^{34}SO_4^{2-}$, adapted from *Krouse and Grinenko*, [1991].

Under some environmental conditions, isotopic fractionation processes may be treated as taking place in an open system – essentially a case in which the reservoir of reactant species can be assumed inexhaustible. In this case, the $\delta$ of the product species will be offset from that of the reactant species by the kinetic isotopic enrichment factor, $\varepsilon$, such that $\delta = \delta_o + \varepsilon$.

### 1.4.4 Sulfur Isotopes in the environment

At the present time, information pertaining to the isotopic composition of atmospheric sulfur species or the isotopic fractionation associated with important

atmospheric processes which affect these species is rather sparse. Sulfur isotopic compositions vary greatly among emission sources, and to a lesser extent with geographical location, although there are still some discernible trends. For example, Figure 1.2 shows that reduced sulfur species generally have lower $\delta^{34}S$ values than species in high oxidation states, and that $\delta^{34}S$ values range from about –30 to +30‰. The $\delta^{34}S$ of seawater sulfate is about + 21‰.

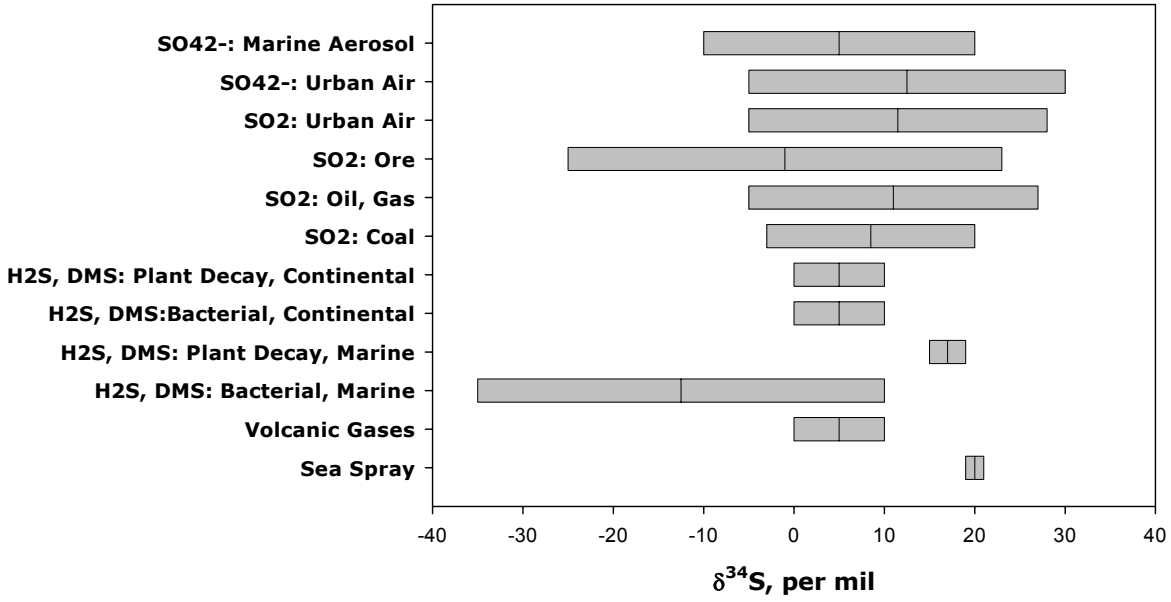


**Figure 1.3**: Sulfur isotopic composition of sulfur-containing compounds in the environment, adapted from *Krouse and Grinenko* [1991]

The discrepancy between the $\delta^{34}S$ is associated with biological reduction processes. The $\delta^{34}S$ of $H_2S$ produced by biogenic activity in wetlands is about 0 to –70 ‰ lower than co-existing sulfate. Though not so pronounced, a similar trend has been found in marine aerosols, where the aerosol sulfate is generally 8-10‰ enriched compared to co-existing gaseous sulfide. Similarly, sulfate found at springs in the Paige

Mountains in Northern Canada were measured to have a $\delta^{34}S$ of about +16‰, compared to –32 to –38 ‰ for $SO_2$ and sulfide found in the same location.

The $\delta^{34}S$ of anthropogenic sulfur sources is considerably less variable. The $\delta^{34}S$ of coal ranges from –30 to +30 ‰, but the flue gas emissions from coal combustion mostly have values of $\delta^{34}S$ between –1 and 3 ‰. Oil and $H_2S$ in gas/oil mixtures are similar, with $\delta^{34}S$ values generally between 0-10 ‰. Sulfide ores vary between $\delta^{34}S$ = -25‰ and $\delta^{34}S$ = +25‰, but commonly have values of $\delta^{34}S$ of about 0 to 5‰. Atmospheric OCS is estimated to have an average $\delta^{34}S$ of 11‰.

There are very few measurements of the isotopic compositions of stratospheric sulfate aerosols. To our knowledge, only one comprehensive data set exists. Pronounced and dramatic increases in the SSA loading were observed for about 3 months immediately following the eruption following the 1963 eruption at Mt. Agung, Bali, Indonesia [*Castleman et al.*, 1973; *Castleman et al.*, 1974]. After a pronounced increase in $\delta^{34}S$ that preceded the maximum SSA loading, $\delta^{34}S$ dipped to negative values before a gradually relaxing of the aerosol isotopic signature to nominal background levels. This effect can be seen at all latitudes and altitudes that were sampled (See Chapter 4). The steady-state background aerosol in the Junge Layer appears to have an average value of $\delta^{34}S \sim +2.3$ ‰.

### 1.4.5 Short note on mass-independent isotopic effects

Up to this point, we have addressed mass-dependent isotopic effects, and dealt only with the preferential processing between $^{34}S$ and $^{32}S$. Under normal circumstances, the fractionation of the heavy isotopes (in the case of sulfur $^{33}S$, $^{34}S$ and $^{36}S$) are not

independent, and occurs as predicted by theory. The ratio between $^{33}S$ and $^{34}S$ fractionation ratios is 0.515. However, deviations, which are expressed as $\Delta$, where $^{33}\Delta = \delta^{34}S - 0.515\ \delta^{33}S$ near the origin, are often observed.

Mass-independent isotopic effects refer to deviations from the expected mass-dependent behavior. These deviations were first observed by Thiemens and Heidenreich in the production of ozone from oxygen where the isotopic discrimination between $^{18}O$ and $^{16}O$ did not follow a conventional mass-dependence [*Thiemens and Heidenreich*, 1983].

Many explanations have been advanced to explain these effects. [*Weston*, 1999] has provided a thorough review of the literature on this subject. There is at present no theoretically rigorous explanation for mass-independent isotopic effects, although an RRKM (Rice, Ramsperger, Kassel, and Marcus)-based theory has been recently been used to successfully predict the experimentally observed mass-independent isotopic effects in the formation of ozone from $O_2$ and O [*Gao and Marcus*, 2001]. In the framework of this RRKM-based theory, the "mass-independent" isotope effects that are associated with the formation of $O_3$ is attributed to differences in how energy can be redistributed between the rovibrational states in the pre-equilibrium states and in the exit channels available for the production of the different isotopomers [*Gao and Marcus*, 2001].

In several recent studies, mass-independent effects in sulfur-containing compounds have been applied to geophysical questions [*Colman et al.*, 1996; *Farquhar et al.*, 2001; *Thiemens*, 1999]. However, given the uncertainty surrounding the origins of

these apparent mass-independent effects coupled with the difficulty of their measurement, these effects are not utilized in this work.

**References**

Canfield, D.E., Biogeochemistry of sulfur isotopes, in *Reviews in Mineralogy and Geochemistry: Stable Isotope Geochemistry*, edited by J.W. Valley, and D.R. Cole, pp. 607-636, Mineralogical Society of America, 2001.

Carslaw, K.S., S.L. Clegg, and P. Brimblecombe, A thermodynamic model of the system HCl-$HNO_3$-$H_2SO_4$-$H_2O$, including solubilities of HBr, from <200 to 328 K, *J. Phys. Chem.*, *99*, 11557-11574, 1995.

Carslaw, K.S., T. Peter, and S.L. Clegg, Modeling the composition of liquid stratospheric aerosols, *Rev. Geophys.*, *35*, 125-154, 1997.

Castleman, J.A.W., H.R. Munkelwitz, and B. Manowitz, Contribution of volcanic sulphur compounds to the stratospheric aerosol layer, *Nature*, *244*, 345-346, 1973.

Castleman, J.A.W., H.R. Munkelwitz, and B. Manowitz, Isotopic studies of the sulfur component of the stratospheric aerosol layer, *Tellus*, *26*, 222-234, 1974.

Chin, M., and D.D. Davis, A reanalysis of carbonyl sulfide as a source of stratospheric background sulfur aerosol, *J. Geophys. Res.*, *100*, 8993-9005, 1995.

Clegg, S.L., and P. Brimblecombe, Application of a multi-component thermodynamic model to activities and thermal properties of 0-40 mol $kg^{-1}$ aqueous sulfuric acid from <200 to 328 K, *J. Chem. Eng. Data*, *40*, 43-64, 1995.

Clegg, S.L., P. Brimblecombe, and A.S. Wexler, Thermodynamic model of the system $H^+$-$NH_4^+$-$SO_4^{2-}$-$NO_3$-$H_2O$ at tropospheric temperatures, *J. Phys. Chem.*, *102*, 2137-2154, 1998.

Colman, J.J., X.P. Xu, M.H. Thiemens, and W.C. Trogler, Photopolymerization and mass-independent sulfur isotope fractionations in carbon disulfide, *Science*, *273*, 774-776, 1996.

Crutzen, P.J., The possible importance of CSO for the sulfate aerosol layer of the stratosphere, *Geophys. Res. Lett.*, *3*, 73-76, 1976.

Farquhar, G.D., J.R. Ehleringer, and K.T. Hubick, Carbon isotopic discrimination and photosynthesis, *Ann. Rev. Plant Phys. Plant. Mol. Bio.*, *40*, 503-537, 1989.

Farquhar, J., J. Savarino, S. Airieau, and M.H. Thiemens, Observation of wavelength-sensitive mass-independent sulfur isotope effects during $SO_2$ photolysis: Implications for the early atmosphere, *J. Geophys. Res. - Planets*, *106*, 32829-32839, 2001.

Farwell, S.O., D.L. MacTaggart, W. Chathan, D.O. Everson, K. Samaranayake, and Y.T. Lim, Airborne measurements of total sulfur gases during NASA Global Tropospheric Experiment/Chemical Instrumentation Test and Evaluation 3., *J. Geophys. Res.*, *100*, 7223-7234, 1995.

Forrest, J., and L. Newman, Sampling and analysis of atmospheric sulfur compounds for isotope ratio studies, *Atmos. Environ.*, *7*, 561-573, 1973.

Forrest, J., and L. Newman, Silver-110 microgram sulfate analysis for the short time resolution of ambient levels of sulfur aerosol, *Anal. Chem.*, *49*, 1579-1584, 1977.

Gao, Y.Q., and R.A. Marcus, Strange and unconventional isotope effects in ozone formation, *Science*, *293*, 259-263, 2001.

Goldman, A., M.T. Coffey, T.M. Stephen, C.P. Rinsland, W.G. Mankin, and J.W. Hannigan, Isotopic OCS from high-resolution balloon-borne and ground-based infrared absorption spectra, *J. Quant. Spectros. Rad. Trans.*, *67*, 447-455, 2000.

Golombek, A., and R.G. Prinn, A Global Three-Dimensional Model of the Stratospheric Sulfuric Acid Layer, *J. Atmos. Chem.*, *16*, 179-199, 1993.

Graf, H.F., J. Feichter, and B. Langmann, Volcanic sulfur emissions: Estimates of source strength and its contribution to the global sulfate distribution, *J. Geophys. Res.*, *102*, 10727-10738, 1997.

Griffith, D.W.T., N.B. Jones, and W.A. Matthews, Interhemispheric ration and annual cycle of carbonyl sulfide (OCS) total column from ground-based solar FTIR, *J. Geophys. Res.*, *103*, 8447-8454, 1998.

Griffith, D.W.T., G.C. Toon, B. Sen, J.F. Blavier, and R.A. Toth, Vertical profiles of nitrous oxide isotopomer fractionation measured in the stratosphere, *Geophys. Res. Lett.*, *27*, 2485-2488, 2000.

Hamill, P., E.J. Jensen, P.B. Russell, and J.J. Bauman, The life cycle of stratospheric aerosol particles, *Bull. Am. Meteor. Soc.*, *78*, 1395-1410, 1997.

Hervig, M., and T. Deshler, Evaluation of aerosol measurements from SAGE II, HALOE, and balloonborne optical particle counters, *J. Geophys. Res.*, *107*, art. no. 4031, 2002.

Hitchman, M.H., M. McKay, and C.R. Trepte, A climatology of stratospheric aerosol, *J. Geophys. Res.*, *99*, 20689-20700, 1994.

Hoffmann, G., J. Jouzel, and V. Masson, Stable water isotopes in atmospheric general circulation models, *Hydrological Processes*, *14*, 1385-1406, 2000.

Hoffmann, M.R., and J.G. Calvert, Chemical transformation modules for Eulerian acid deposition models, Volume II: the aqueous-phase chemistry, pp. 155, NCAR, Boulder, Colorado, 1985.

Hoffmann, M.R., and D.J. Jacob, Kinetics and mechanisms of the catalytic oxidation of dissolved sulfur dioxide in aqueous solution: an application to nighttime fog water chemistry, in *$SO_2$, NO and $NO_2$ Oxidation Mechanisms: Atmospheric Considerations*, edited by J.G. Calvert, pp. 101-172, Butterworth Publishers, Boston, 1984.

Hofmann, D.J., Aircraft sulphur emissions, *Nature*, *349*, 659, 1991.

Hofmann, D.J., R.S. Stone, M.E. Wood, T. Deschler, and J.M. Harris, An analysis of 25 yearsof balloonborne aerosol data in search of a signature of the subsonic commerial aircraft fleet, *Geophys. Res. Lett.*, *25*, 2433-2436, 1998.

Johnson, M.S., G.D. Billing, A. Gruodis, and M.H.M. Janssen, Photolysis of nitrous oxide isotopomers studied by time-dependent hermite propagation, *J. Phys. Chem. A*, *105*, 8672-8680, 2001.

Jouzel, J., R.D. Koster, R.J. Suozzo, G.L. Russell, J.W.C. White, and W.S. Broeker, Simulations of the HDO and $H_2O$-$^{18}O$ atmospheric cycles using the NASA GISS general-circulation model - sensitivity experiments for present-day conditions, *J. Geophys. Res. - Atmospheres*, *96*, 7495-7507, 1991.

Junge, C.E., C.W. Chagnon, and J.E. Manson, Stratospheric Aerosols, *J. Meteorology*, 81-108, 1961.

Kjellstrom, E., A Three dimensional global model study of carbonyl sulfide in the troposphere and the lower stratosphere, *J. Atmos. Chem.*, *29*, 151-177, 1998.

Krouse, H.R., and V.A. Grinenko, editors, *Stable Isotopes: Natural and Anthropogenic sulphur in the Environment, Scope 43*, 400 pp., John Wiley and Sons, 1991.

Lazrus, A.L., B. Gandrud, and R.D. Cadle, Chemical composition of air filtration samples of the stratospheric sulfate layer, *J. Geophys. Res.*, *76*, 8083-8088, 1971.

Love, S.G., and D.E. Brownlee, A direct measurement of the terrestrial mass accretion rate of cosmic dust, *Science*, *262*, 550-553, 1993.

Lukachko, S.P., I.A. Waitz, R.C. Miake-Lye, R.C. Brown, and M.R. Anderson, Production of sulfate aerosol precursors in the turbine and exhaust nozzle of an aircraft engine, *J. Geophys. Res.*, *103*, 16159-16174, 1998.

Martin, L.R., Kinetic studies of sulfite oxidation in aqueous solution, in *$SO_2$, NO and $NO_2$ oxidation Mechanisms: atmospheric considerations*, edited by J.G. Calvert, pp. 63-100, Butterworth Publishers, Boston, 1984.

McArdle, J.V., and M.R. Hoffmann, Kinetics and mechanism of the oxidation of aquated sulfur dioxide by hydrogen peroxide at low pH, *J. Phys. Chem.*, *87*, 5425-5429, 1983.

Michelson, H.A., A parameterization for the activity of H+ in aqueous aulfuric acid solutions, *Geophys. Res. Lett.*, *25*, 3571-3573, 1998.

Miller, C.E., and Y.L. Yung, Photo-induced isotopic fractionation, *J. Geophys. Res.*, *105*, 29039-29051, 2000.

Murphy, D.M., D.S. Thomson, and M.J. Mahoney, In Situ Measurements of Organics, Meteoretic Material, Mercury, and Other Elements in Aerosols at 5 to 19 Kilometers, *Science*, *282*, 1664-1669, 1998.

Pantani, M., M.D. Guasta, D. Guzzi, and L. Stefanutti, Polar stratospheric clouds of liquide aerosol: an experimental determinationof mean size distribution, *J. Aerosol. Sci.*, *30*, 559-567, 1999.

Pitari, G., E. Mancini, V. Rizi, and D.T. Shindell, Impact of future climate and emission changes on stratospheric aerosols and ozone, *J. Atmos. Sci.*, *59*, 414-440, 2002.

Pueschel, R.F., Stratospheric aerosols:formation, properties, effects, *J. Aerosol. Sci.*, *27*, 383-402, 1995.

Rahn, T., and M. Wahlen, Stable isotope enrichment in stratospheric nitrous oxide, *Science*, *278*, 1776-1778, 1997.

Rahn, T., and M. Wahlen, A reassessment of the global isotopic budget of atmospheric nitrous oxide, *Global Biogeochemical Cycles*, *14*, 537-543, 2000.

Robinson, P.J., and K.A. Holbrook, *Unimolecular reactions*, chapter 9 pp., Wiley, London, 1972.

Robock, A., Volcanic eruptions, in *Encyclopedia of Global Environmental Change*, edited by M. M.C., and J.S. Perry, pp. 738-744, John Wiley & Sons, Chichester, 2002.

Seinfeld, J.H., and S.N. Pandis, *Atmospheric Chemistry and Physics: From Air Pollution to Climate Change*, 1326 pp., John Wiley and Sons, New York, New York, 1998.

Steele, H.M., and P. Hamill, Effects of temperature and humidity on the growth and optical properties of sulfuric acid-water droplets in the stratosphere, *J. Aerosol. Sci.*, *12*, 517-528, 1981.

Thiemens, M.H., Atmosphere science - Mass-independent isotope effects in planetary atmospheres and the early solar system, *Science*, *283*, 341-345, 1999.

Thiemens, M.H., and J.E. Heidenreich, The Mass-independent fractionation of oxygen - a novel isotope effect and its possible cosmochemical implications, *Science*, *219*, 1073-1075, 1983.

Thomason, L.W., G.S. Kent, C.R. Trepte, and L.R. Poole, A comparison of the stratospheric aerosol background periods of 1979 and 1989-1991, *J. Geophys. Res.*, *102*, 3611-3616, 1997.

Timmreck, C., Three-dimensional simulation of stratospheric background aerosol: First results of a multi-annual general circulation model simulation, *J. Geophys. Res.*, *106*, 28313-28332, 2001.

Turco, R.P., R.C. Whitten, and O.B. Toon, Stratospheric aerosols: observations and theory, *Rev. Geophys. and Space Physics*, *20*, 233-279, 1982.

Turco, R.P., R.C. Whitten, O.B. Toon, J.B. Pollack, and P. Hamill, OCS, stratospheric aerosols and climate, *Nature*, *283*, 283-286, 1980.

Watts, S.F., The mass budgets of carbonyl sulfide, dimethyl sulfide, carbon disulfide and hydrogen sulfide, *Atmos. Environ.*, *34*, 761-779, 2000.

Weisenstein, D.K., Personal Communication, 2002.

Weisenstein, D.K., G.K. Yue, M.K.W. Ko, N.-D. Sze, J.M. Rodriguez, and C.J. Scott, A two-dimensional model of sulfur species and aerosols, *J. Geophys. Res.*, *102*, 13019-13035, 1997.

Weston, J.R.E., Anomalous or mass-independent isotope effects, *Chem. Rev.*, *99*, 2115-2136, 1999.

Yakir, D., and L. da Silveira Lobo Sternberg, The used of stable isotopes to study ecosystem gas exchange, *Oecologia*, *123*, 297-311, 2000.

Yue, G.K., L.R. Poole, P.-H. Wang, and E.W. Chiou, Stratospheric aerosol acidity, density, and refractive index deduced form SAGE II and NMC temperature data, *J. Geophys. Res.*, *99*, 3727-3738, 1994.

Yung, Y.L., and C.E. Miller, Isotopic fractionation of stratospheric nitrous oxide, *Science*, *278*, 1778-1780, 1997.

Zhang, H., P.O. Wennberg, V.H. Wu, and G.A. Blake, Fractionation of $^{14}N^{15}N^{16}O$ and $^{15}N^{14}N^{16}O$ during photolysis at 213 nm, *Geophys. Res. Lett.*, *27*, 2481-2484, 2000.

## Appendix A.1 Sulfur Chemical and Photochemical pathways under atmospheric conditions

### A.1.1 Aqueous phase chemistry sulfur chemistry

The relative importance of homogeneous and heterogeneous oxidative pathways for sulfur compounds depends of a range of climatological and microphysical factors, including relative humidity, sunlight intensity, and aerosol concentration and size distribution [*Hoffmann and Jacob*, 1984]. A rudimentary understanding of aqueous-phase oxidative pathways for S(IV) are especially in the context of the discussion in Chapter 6.

$SO_2$ dissolved in aqueous solution can be oxidized by a host of pathways, the most important being oxidation by $O_3$, $H_2O_2$, $O_2$ via metal catalysis with iron and manganese, OH, and in some cases, $NO_2$.

### A.1.2 $SO_2$ oxidation by $O_3$

$SO_2$ oxidation by $O_3$ in the gas phase is very slow. However, in aqueous solution, the oxidation of S(IV) to S(VI) by $O_3$ can proceed rapidly. From experimental data, a mechanism has been determined:

$$-\frac{d[S(IV)]}{dt} = (k_o[SO_2 \bullet H_2O] + k_1[HSO_3-] + k_2[SO_3^{2-}])[O_3] \qquad \text{(A.1.1)}$$

where $k_0 \approx 2.4 \pm 1.1 \times 10^4$ $M^{-1}s^{-1}$; $k_1 \approx 3.1 \pm 0.7 \times 10^5$ $M^{-1}s^{-1}$, and $k_2 \approx 2.4 \pm 1.1 \times 10^9$ $M^{-1}s^{-1}$ [*Seinfeld and Pandis*, 1998].

There is a complex dependence of the reaction rate on pH brought upon by the speciation of the sulfur species [*Hoffmann and Calvert*, 1985; *Seinfeld and Pandis*, 1998]. At ambient ozone concentrations of ~ 30 ppbv, the rate of heterogenous oxidation

by this mechanism varies between ~0.01% $SO_2(g)$ $h^{-1}$ at pH 2 to 7000% $SO_2(g)$ $h^{-1}$ at pH 6. The reaction is therefore important above ~ pH 4. The strong pH dependence of the reaction makes it self-limiting. Because stratospheric aerosols are very acidic, we expect that this oxidative pathway is relatively unimportant in stratospheric $SO_2$ processing.

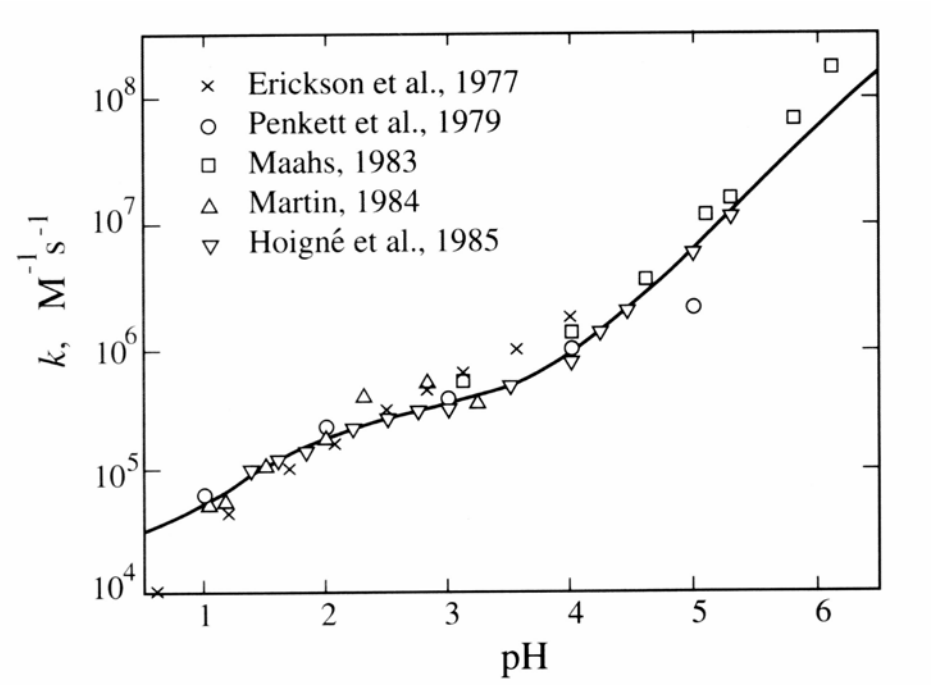


**Figure A.1.1:** pH dependence of $SO_2$ oxidation by $O_3$. Figure from Seinfeld and Pandis (1998)

### A.1.3 $SO_2$ oxidation by $H_2O_2$

In contrast, the rate of oxidation of $SO_2$ by $H_2O_2$ increases with increasing pH except at pH < 2.5 and tends to dominate other aqueous oxidative pathways at low pH (Figure A.1.2.) [*Hoffmann and Jacob*, 1984; *Martin*, 1984].

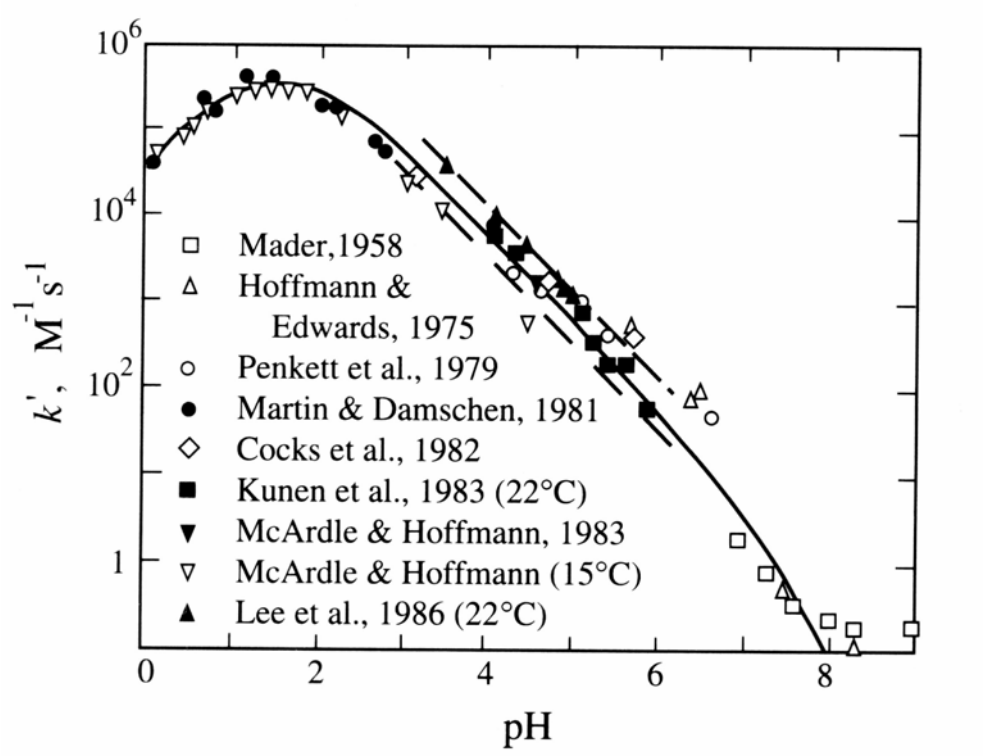


**Figure A.1.2:** pH dependence of $SO_2$ oxidation by $H_2O_2$. Figure from Seinfeld and Pandis (1998)

The fitted data yield the expression:

$$-\frac{d[S(IV)]}{dt} = \frac{k[H^+][H_2O_2][HSO_3^-]}{1+K[H^+]} \qquad \text{(A.1.2)}$$

where $k \approx 5.5 \times 10^7$ $M^{-1}s^{-1}$ and K = 113 $M^{-1}$ at 298 K [*Hoffmann and Calvert*, 1985; *Seinfeld and Pandis*, 1998]. Hoffmann and Edwards (1975) proposed a mechanism consistent with experimental measurements, which proceeds via equilibrium with a peroxymonosulfurous acid ion, and in which the second step increases as pH decreases [*McArdle and Hoffmann*, 1983; *Seinfeld and Pandis*, 1998].

$$HSO_3^- + H_2O_2 \underset{k_{-1}}{\overset{k_1}{\rightleftharpoons}} SO_2OOH^- + H_2O \qquad \text{(A.1.3)}$$

$$SO_2OOH^- + H^+ \xrightarrow{k_2} H_2SO_4 \qquad (A.1.4)$$

### A.1.4 $SO_2$ oxidation by OH radical

Oxidation of OH radicals may be significant in the aqueous phase as well as in the gas phase, since OH and $HO_2$ can be scavenged heterogeneously from the gas phase [*Seinfeld and Pandis*, 1998]. The oxidation pathway, as depicted in Figure A.1.3, is rather complicated, and involves a chain reaction in which multiple sulfate ions are produced from a single OH attack.

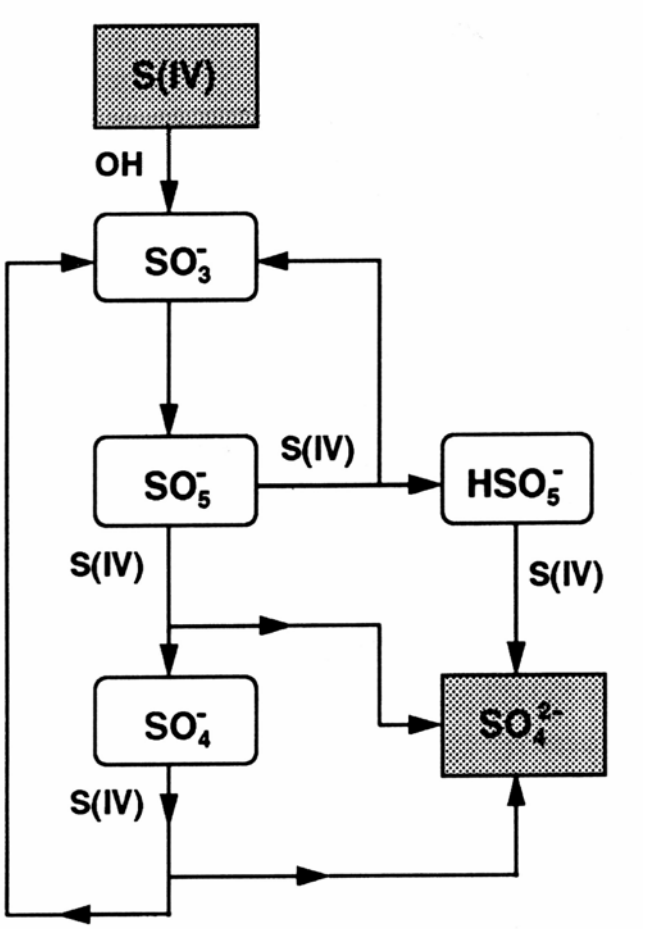


**Figure A.1.3:** Mechanism for the oxidation of S(IV) by OH radical. Figure taken from Seinfeld and Pandis (1998).

The net rate of sulfur oxidation can be expressed as:

$$\frac{-d[S(IV)]}{dt} = k_1[SO_5^-][HSO_3^-] + k_2[SO_4^-][HSO_3^-] + k_3[HSO_5^-][HSO_3^-][H^+] \quad \text{(A.1.5)}$$

where $k_1$, $k_2$, and $k_3$ are the rate constants associated with the elementary reactions:

$$SO_5^- + HSO_3^- \rightarrow SO_4^- + SO_4^{2-} + H^+ \qquad k_1 = 7.5 \times 10^4\ M^{-1}s^{-1} \qquad (1)$$

$$SO_4^- + HSO_3^- \rightarrow SO_4^{2-} + SO_3^- + H^+ \qquad k_2 = 7.5 \times 10^8\ M^{-1}s^{-1} \qquad (2)$$

$$HSO_5^- + HSO_3^- + H^+ \rightarrow 2SO_4^{2-} + 3H^+ \qquad k_3 = 7.1 \times 10^6\ M^{-1}s^{-1} \qquad (3)$$

respectively, and where the concentrations of the intermediates can be determined by assuming a pseudo-steady state for the system.

### A.1.5 $SO_2$ oxidation by $O_2$ via metal catalysis

The oxidation of $SO_2$ by $O_2$ in the absence of a catalyst is negligible. However, ferric iron (Fe(III)) or manganese in the Mn(II) oxidation state will catalyze this reactions. The mechanisms invoked to explain this type of metal catalysis generally involve inner-sphere complexation of the catalytic metal by the sulfite followed by binding of $O_2$ by the complex. The mechanisms involve successive 2-electron transfers. These catalytic reactions have complex pH dependences and expressions of empirical rate laws are cumbersome. In addition, there appears to be a synergistic effect between manganese and iron catalysis of $SO_{2(aq)}$ oxidation by $O_2$. At pH 3 and [S(IV)] < 10 μM, the expression (A.1.6):

$$\frac{-d[S(IV)]}{dt} = 750[Mn(II)][S(IV)] + 2600[Fe(III)][S(IV)] + 1\times10^{10}[Mn(II)][Fe(III)][S(IV)]$$

holds. For a comprehensive review of the subject, the reader is referred to Hoffmann and Jacob (1985) and Seinfeld and Pandis (1998).

### A.1.6 $SO_2$ oxidation by nitrogen oxides

Because $NO_2$ is not very soluble in water, oxidation of S(IV), via the pathway below, is not particularly important except under unusual circumstances such as fogs in highly polluted urban areas in which there are elevated levels of $NO_2$.

$$2NO_2 + HSO_3^- \xrightarrow{H_2O} 3H^+ + 2NO_2^- + SO_4^{2-} \qquad \text{(A.1.7)}$$

The oxidation rate in this case can be expressed as:

$$\frac{-d[S(IV)]}{dt} = k[S(IV)][NO_2] \qquad \text{(A.1.8)}$$

where $k$ is pH dependent, having a value of $1.4 \times 10^5$ $M^{-1}s^{-1}$ at pH 5 and about an order of magnitude higher at pH 6 [*Seinfeld and Pandis*, 1998].

## Appendix 1.2 Homogeneous sulfur chemistry

OCS and $SO_2$ are considered important precursors of SSA particles. DMS, a major component in the global sulfur budget, is oxidized by reaction with OH and $NO_3$ to $SO_2$. OCS is either produced directly by marine bio-organisms or as the result of oxidation of $CS_2$ by OH.

$$CS_2 + OH \rightarrow OCS + SH \qquad \text{(A.1.9)}$$

OCS is relatively unreactive in the troposphere. Oxidation pathways involving O and OH are minor loss pathways (Table A.1.1).

**Table A.1.1: Reaction rate constants for homogeneous OCS reactions**

| Reaction | $k$(T)=Ae$^{-Ea/RT}$, molecules cm$^{-3}$ s$^{-1}$ | $k$(T= 298.15 K) (molecules cm$^{-3}$ s$^{-1)}$ |
|---|---|---|
| OCS + O → CO + SO | $2.1\times10^{-11}e^{-2200/T}$ | $1.3\times10^{-14}$ |
| OCS + OH → $CO_2$ + HS | $1.1\times10^{-13}e^{-1200/T}$ | $1.9\times10^{-15}$ |

SO and HS are further processes to $SO_2$ and eventually to $SO_4^{2-}$. The complete set of gas phase reactions is presented in Table 6.2.

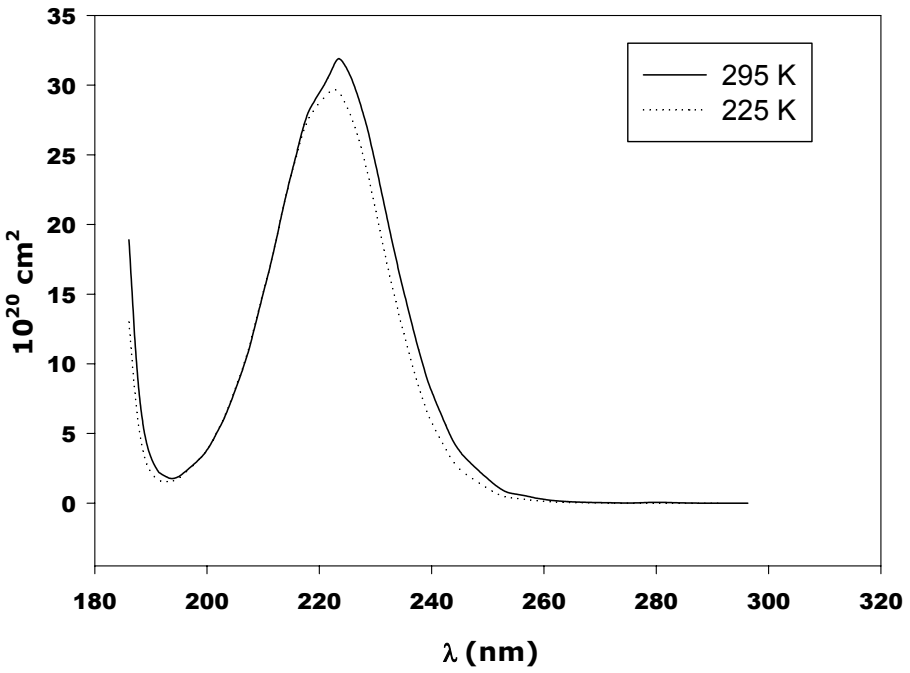


**Figure A.1.4:** Absorption Cross-sections for OCS, after DeMore et al., 1997.

The primary mechanism by which OCS is lost in the stratosphere is photolysis to CO and S. As shown in Figure A.1.4, the absorption cross-sections for OCS vary with temperature, especially on the red side of the absorption maximum.